CEPT ECC
Electronic Communications Committee

ECC Report 349

Unwanted emissions of IRIDIUM NEXT satellites in the band 1610.6-1613.8 MHz, monitoring campaign of November 2020 to May 2021

approved 3 February 2023

0 EXECUTIVE SUMMARY

This Report describes measurements and simulation results of IRIDIUM NEXT's unwanted emissions into the radio astronomy (RAS) band 1610.6-1613.8 MHz. The measurements were carried out from November 2020 to May 2021 and are part of a recurring monitoring program of this RAS band as requested by Decides 5 of ECC Decision (09)02 [6]. In the framework of SAT MoU, the Leeheim space radio monitoring station (Germany) measured 16 satellites of IRIDIUM's second-generation MSS network.

The measurement setup and calibration was developed in ECC Report 171 [7] and ECC Report 226 [8], and further refined. Initial measurements taken on a few IRIDIUM replacement satellites ("IRIDIUM NEXT") in 2017 revealed some problems with the noise characterisation and the measurement sensitivity of the Leeheim equipment, due to the lower emissions observed at that time. Thus, the measurement methods and software modules were revised in 2019 and 2020 to improve accuracy and sensitivity in the case of lower observed emissions. These are described in ECC Report 247 [9].

The satellite unwanted emissions data collected by BNetzA (German Federal Network Agency) Leeheim Space Radio Monitoring Station during 2020 and 2021 was examined and processed following the procedure described in ECC Report 247. The results are shown on Table 1, together with the results of previous campaigns.

In addition to the estimate of data loss, a DEC value shows the estimated further reduction in unwanted emissions that would be necessary to achieve the target 2% data loss. To overcome the limitations in sensitivity, data loss and DEC values were calculated for the system noise (using the void satellite passes) and these were subtracted from the measurement results.

Table 1: Results of IRIDIUM NEXT measurement campaigns

	Nov. 2013		April/May 2019		Oct./Nov. 2019		Nov. 2020/May 2021	
	Data loss	DEC (dB)	Data loss	DEC (dB)	Data loss	DEC (dB)	Data loss	DEC (dB)
Measurement	IRIDIUM + Noise							
1613.8 MHz	*	*	48.00%	18.7	100%	31.8	99.90%	24.7
1610.6 MHz	*	*	26.40%	15.7	100%	24.7	37.20%	16.7
Noise	Noise							
1613.8 MHz	*	*	18.70%	15.7	15.60%	18.2	17.50%	15.7
1610.6 MHz	*	*	21.70%	16.7	7.20%	10.1	18.50%	11.6
Result	IRIDIUM							
1613.8 MHz	100%	32.3	29.30%	3	84.40%	13.6	82.50%	9.1
1610.6 MHz	94.4%	22.8	4.70%	-1	92.70%	14.6	18.80%	5.1

* In 2013, Leeheim did not take noise measurements to compensate for elevation-variable antenna noise.

Table 1 results for four different measurement campaigns, beginning with the first-generation constellation (2013 [8]) and then the second-generation satellites under different operating settings (April 2019, October 2019 and May 2021). IRIDIUM reported that the settings used in April 2019 were too restrictive for their operations; measurements taken in October 2019 reflect the situation with restrictions removed. New operational restrictions were implemented in May 2020 and were in place when the most recent measurements were taken.

The results show, in regard to the reduction of unwanted emissions, an improvement over the results from October/November 2019, but they are still less satisfactory compared to the measurements made in April/May 2019 (when IRIDIUM had significantly reduced traffic on satellites in the vicinity of European RAS stations, such as Effelsberg). It should be noted that ECC Report 247 [9] concludes that “because of the noise of the measurement chain, it may not be possible to assess data loss performance down to the 2% objective”. Therefore, “in order to assess the sensitivity of the measurement chain, users may use data taken from several ‘void satellite passes’, i.e. without pointing towards IRIDIUM satellites, and assess data loss on that basis”. By comparing the data loss values of the results of the epfd simulation for both cases (i.e., with and without IRIDIUM signals, both subject to receiver noise), one can infer the actual impact of the satellites alone. The same can be done for the so-called DEC parameter, which is the estimated attenuation of the interference level needed to reach the 2% target.

It is noted that the data loss (percentage) and the DEC value (dB) are not linearly related, due to the fact that "data loss" is defined as a binary outcome. Interference above the threshold, after averaging over the reference 2000 s time period, is classified as a "data loss" event, regardless of whether the exceedance is 0.1 dB or 20 dB. As average emissions are reduced close to the threshold, the data loss has been shown to fall more significantly. The DEC metric was therefore considered a more effective measure of exceedance.

TABLE OF CONTENTS

LIST OF ABBREVIATIONS

Abbreviation	Explanation
BNetzA	Federal Network Agency (Germany)
CEPT	European Conference of Postal and Telecommunications Administrations
ECC	Electronic Communications Committee
epfd	Equivalent Power Flux Density
FDMA	Frequency Division Multiple Access
FMDA	Frequency Division Multiple Access
HPAs	High-Power Amplifiers
ITU	International Telecommunications Union
LEO	Low Earth Orbit
MSS	Mobile Satellite Service
OH	Hydroxyl radical
PFD	Power Flux Density
r.s.s	Root Sum of Squares
RAS	Radio Astronomy Service
SAW	Surface Acoustic Wave
SPFD	Spectral Power Flux Density
T/R	Transmit/Receive
TDD	Time-Division Duplex
TDMA	Time Division Multiple Access
WRC	World Radiocommunication Conference

1 INTRODUCTION

WARC-1992 created new allocations for the mobile-satellite service (MSS) (space-to-Earth) in 1613.8 - 1626.5 MHz, and the radio astronomy service (RAS) in 1610.6-1613.8 MHz. The unwanted emissions of IRIDIUM satellites falling in the radio astronomy (RAS) band 1610.6-1613.8 MHz have previously been documented in ECC Report 171 [7] and ECC Report 226 [8]. In November 2012, ECC amended its ECC Decision (09)02 to include a new Decides 5, stating:

- *"that the compliance with the conditions for use of radio frequencies by current and future MSS systems in the band 1613.8-1626.5 MHz (space-to-Earth) and the degree of interference in the frequency band 1610.6-1613.8 MHz caused by this usage shall be monitored regularly (e.g. once a year) by a competent body and the results be reported to the ECC;"*

The purpose of Decides 5 is to compare measurements over several years and show possible changes in the interference situation due to changes of the satellite configuration, parameters or traffic load.

The international satellite monitoring station in Leeheim was tasked to measure the unwanted emissions of a selection of IRIDIUM NEXT satellites, the second generation of IRIDIUM satellites. The original IRIDIUM satellite constellation was replaced with a new constellation during the period 2017-2019, and the old satellites were deorbited. Amongst other objectives, the new satellites were designed to reduce the levels of unwanted emissions falling to the RAS band. In the NORAD catalogue of satellite objects[1], the first generation satellites carried two-letter designations (IRIDIUM-XX), while the IRIDIUM Next satellites carry three-letter designations (IRIDIUM-1xx).

This Report contains measurements carried out by the Leeheim space radio monitoring station (Germany) between November 2020 and May 2021. The measurement results were used in a simulation tool to assess the equivalent power flux density (epfd) generated in the RAS band, and the resulting data loss is compared with the results in ECC Report 171 [7] and ECC Report 226 [8] and with measurements taken by Leeheim in 2019.

The following conditions were applied for the measurements and their processing:

- Satellites and times of monitoring were chosen to meet the requirements described in the LS to SAT MoU ([10]) on IRIDIUM measurements ("Requested measurements on Operational IRIDIUM NEXT constellation"). This refers to 16 measurements split into 2 measurement periods. The measurements in period 1 and 2 were taken in November and December 2020, and in March to May 2021, respectively. Both measurement sets comprise a total of 8 measurements each. In both periods, the same satellites where measured for an even and odd plane (plane 2 and 3). Furthermore, each chosen satellite was measured during day and night passes, which leads to a total of 4 measurement on each of the 4 satellites under investigation;
- The evaluation was based on the software tool as described in ECC Report 247 ("Description of the software tool for processing of measurements data of IRIDIUM satellites at the Leeheim station"). The latest version of the DataReduction MATLAB tool was used for the calculations.

[1] NORAD (North American Aerospace Defense Command) maintains a catalogue of man-made space objects, which is publicly accessible via https://celestrak.org/.

2 DEFINITIONS

Term	Definition
DEC	Estimated further reduction in unwanted emissions that would be necessary to achieve the target 2% data loss

3 MSS AND RAS FREQUENCY ALLOCATIONS

Table 2: Frequency allocations in the band 1610-1626.5 MHz (ITU Radio Regulations, Volume 1 - Articles, Edition of 2020 [1])

Region 1	Region 2	Region 3
1610-1610.6 MOBILE-SATELLITE (Earth-to-space) 5.351A AERONAUTICAL RADIONAVIGATION	**1610-1610.6** MOBILE-SATELLITE (Earth-to-space) 5.351A AERONAUTICAL RADIONAVIGATION RADIODETERMINATION-SATELLITE (Earth-to-space)	**1610-1610.6** MOBILE-SATELLITE (Earth-to-space) 5.351A AERONAUTICAL RADIONAVIGATION Radiodetermination-satellite (Earth-to-space)
5.341 5.355 5.359 5.364 5.366 5.367 5.368 5.369 5.371 5.372	5.341 5.364 5.366 5.367 5.368 5.370 5.372	5.341 5.355 5.359 5.364 5.366 5.367 5.368 5.369 5.372
1610.6-1613.8 MOBILE-SATELLITE (Earth-to-space) 5.351A RADIO ASTRONOMY AERONAUTICAL RADIONAVIGATION	**1610.6-1613.8** MOBILE-SATELLITE (Earth-to-space) 5.351A RADIO ASTRONOMY AERONAUTICAL RADIONAVIGATION RADIODETERMINATION-SATELLITE (Earth-to-space)	**1610.6-1613.8** MOBILE-SATELLITE (Earth-to-space) 5.351A RADIO ASTRONOMY AERONAUTICAL RADIONAVIGATION Radiodetermination-satellite (Earth-to-space)
5.149 5.341 5.355 5.359 5.364 5.366 5.367 5.368 5.369 5.371 5.372	5.149 5.341 5.364 5.366 5.367 5.368 5.370 5.372	5.149 5.341 5.355 5.359 5.364 5.366 5.367 5.368 5.369 5.372
1613.8-1621.35 MOBILE-SATELLITE (Earth-to-space) 5.351A AERONAUTICAL RADIONAVIGATION Mobile-satellite (space-to-Earth) 5.208B	**1613.8-1621.35** MOBILE-SATELLITE (Earth-to-space) 5.351A AERONAUTICAL RADIONAVIGATION RADIODETERMINATION-SATELLITE (Earth-to-space) Mobile-satellite (space-to-Earth) 5.208B	**1613.8-1621.35** MOBILE-SATELLITE (Earth-to-space) 5.351A AERONAUTICAL RADIONAVIGATION Mobile-satellite (space-to-Earth) 5.208B Radiodetermination-satellite (Earth-to-space)
5.341 5.355 5.359 5.364 5.365 5.366 5.367 5.368 5.369 5.371 5.372	5.341 5.364 5.365 5.366 5.367 5.368 5.370 5.372	5.341 5.355 5.359 5.364 5.365 5.366 5.367 5.368 5.369 5.372
1621.35-1626.5 MARITIME MOBILE-SATELLITE (space-to-Earth) 5.373 5.373A MOBILE-SATELLITE (Earth-to-space) 5.351A AERONAUTICAL RADIONAVIGATION Mobile-satellite (space-to-Earth) except maritime mobile satellite (space-to-Earth)	**1621.35-1626.5** MARITIME MOBILE-SATELLITE (space-to-Earth) 5.373 5.373A MOBILE-SATELLITE (Earth-to-space) 5.351A AERONAUTICAL RADIONAVIGATION RADIODETERMINATION-SATELLITE (Earth-to-space) Mobile-satellite (space-to-Earth) except maritime mobile satellite (space-to-Earth)	**1621.35-1626.5** MARITIME MOBILE-SATELLITE (space-to-Earth) 5.373 5.373A MOBILE-SATELLITE (Earth-to-space) 5.351A AERONAUTICAL RADIONAVIGATION Mobile-satellite (space-to-Earth) except maritime mobile satellite (space-to-Earth) Radiodetermination-satellite (Earth-to-space)
5.208B 5.341 5.355 5.359 5.364 5.365 5.366 5.367 5.368 5.369 5.371 5.372	5.208B 5.341 5.364 5.365 5.366 5.367 5.368 5.370 5.372	5.208B 5.341 5.355 5.359 5.364 5.365 5.366 5.367 5.368 5.369 5.372

Note that RAS has a primary allocation in the band 1610.6-1613.8 MHz. Two footnotes are applicable:

5.149 "….administrations are urged to take all practicable steps to protect the radio astronomy service from harmful interference"

5.372 Harmful interference shall not be caused to stations of the radio astronomy service using the frequency band 1 610.6-1 613.8 MHz by stations of the radiodetermination-satellite and mobile-satellite services (No. 29.13 applies). The equivalent power flux-density (epfd) produced in the frequency band 1 610.6-1 613.8 MHz by all space stations of a non-geostationary-satellite system in the mobile-satellite service (space-to-Earth) operating in frequency band 1 613.8-1 626.5 MHz shall be in compliance with the protection criteria provided in Recommendations ITU-R RA.769-2 and ITU-R RA.1513-2, using the methodology given in Recommendation ITU-R M.1583-1, and the radio astronomy antenna pattern described in Recommendation ITU-R RA.1631-0. (WRC-19)

Mobile-Satellite Service (MSS) (Earth-to-space) is allocated in the band 1610.0-1626.5 MHz and Mobile-Satellite Service (space-to-Earth) has a secondary allocation in the band 1613.8-1626.5 MHz. Footnote **5.208B** states that Resolution **739** (rev.WRC-19) applies to this band.

4 RADIOASTRONOMY CHARACTERISTICS AND PROTECTION CRITERIA

4.1 RAS OPERATIONS IN THE BAND 1610.6-1613.8 MHZ

The 1610.6-1613.8 MHz band is used for spectral line observations of the hydroxyl radical (OH). The OH transition at rest frequency 1612 MHz is one of the most important spectral lines for RAS, and is listed as such in Recommendation ITU-R RA.314 [12]. OH was the first cosmic radical to be detected at radio frequencies (1963) and continues to be a powerful research tool. In its ground state the OH molecule produces four spectral lines, at frequencies of approximately 1612, 1665, 1667 and 1720 MHz, all of which have been observed in emission and in absorption in our Galaxy, as well as in external galaxies. The study of OH lines provides information on a wide range of astronomical phenomena, e.g. the formation of protostars and the evolution of stars. To interpret most observations made of the OH molecule, it is necessary to measure the relative strength of several of these lines. The loss of the ability to observe any one of these lines will prevent the study of these classes of physical phenomena.

Using current technology, spectral line observations are made using spectrometers that can simultaneously integrate the power in each of a large number of frequency channels (several thousands up to millions) distributed across the observed frequency band. The width and number of channels is usually adapted to the needs of the scientific program. For some cases, very narrow cosmic maser emission or Zeeman splitting of spectral lines demands for resolutions of much less than a kHz.

Observations in the 1612 MHz band are carried out at RAS sites in numerous countries, worldwide. Observations in the 1612 MHz band are sometimes conducted on targets of opportunity, e.g. particularly on objects such as comets, which have been observed to produce transient emissions in this line.

4.2 PROTECTION CRITERIA OF RAS

Recommendation ITU-R RA.769 [4] specifies the protection criteria for radio astronomical observations and provides threshold levels of detrimental interference for primary RAS bands. In the 1610.6-1613.8 MHz band, the threshold pfd limit is 194 dB(W/m^2) per 20 kHz spectrometer channel bandwidth, assuming 0 dBi antenna gain and an integration time of 2000 seconds for the RAS station. Because this band is used only for spectral line observations, the continuum threshold is not considered hereafter. The limits for other integration times and bandwidths scale as the square root of the ratio of the product of time and bandwidth to that of the nominal 2000 s and 20 kHz, as expressed in Recommendation ITU-R RA.769. A shortened integration time will raise the corresponding threshold pfd limit. A scaling of the interference limits according to Recommendation ITU-R RA.769 and the derivation in the astronomical unit Jansky (Jy) can be found in ECC Report 171, annex 4. (reproduced in Annex 1).

To determine the impact of interference from non-GSO systems, the protection criteria and the relevant epfd methodologies are described in Recommendation ITU-R RA.769-2 [4] and Recommendation ITU-R RA.1513-1 [5], as well as in Recommendation ITU-R S.1586-1 [3] for FSS systems and in Recommendation ITU R M.1583-1 [2] for MSS and RNSS systems. In particular, an epfd threshold of -258 dB(W/m^2) per 20 kHz may be derived from the threshold pfd level considering a maximum antenna gain of 64 dBi for an RAS antenna of 100 m diameter and an integration time of 2000 seconds.

Data loss is defined in Recommendation ITU-R RA.1513-1 as “data that have to be discarded because they are contaminated by the aggregate interference, from one or more sources that exceeds the levels of Recommendation ITU-R RA.769”. This “data loss may result from loss of part of the observing band, part of the observing time or from blockage of part of the sky”. Recommendation ITU-R RA.1513-1 recommends “that the percentage of data loss, in frequency bands allocated to the RAS on a primary basis, be determined as the percentage of integration periods of 2000 s in which the average spectral pfd at the radio telescope exceeds the levels defined (assuming 0 dBi antenna gain) in Recommendation ITU-R RA.769”. The 2000 s integration period is a reference duration used in ITU-R Recommendations, but in practice different integration times are used by radio astronomy stations. For the case of a non-geostationary satellite network, the epfd rather than spfd was used, as described in Recommendation ITU-R M.1583.

Recommendation ITU-R RA.1513 [5] recommends a data loss criterion of 2% caused by any single MSS network. This percentage of data loss is considered an average value calculated over all the possible pointing directions of the RAS station (see Recommendation ITU-R M.1583 [2]).

5 IRIDIUM NEXT SYSTEM CHARACTERISTICS

5.1 IRIDIUM NEXT CONSTELLATION DESCRIPTION

The IRIDIUM system employs 66 Low Earth Orbit (LEO) satellites that support user-to-user, user-to-gateway, and gateway-to-gateway communications. The 66 satellites are evenly distributed in six orbital planes with a 86.4° inclination, with one or more in-orbit spare for each orbital plane. Except for planes 1 and 6, the orbital planes are co-rotating planes spaced 31.6° apart. The first and last orbital planes are spaced 22° apart and form a seam where the satellites are counter-rotating. The IRIDIUM satellite constellation is depicted in Figure 1. The satellites orbit at an altitude of 780 km and have an orbital period of approximately 100 min 28 s. The entire constellation is capable of supporting 3168 communications spot beams.

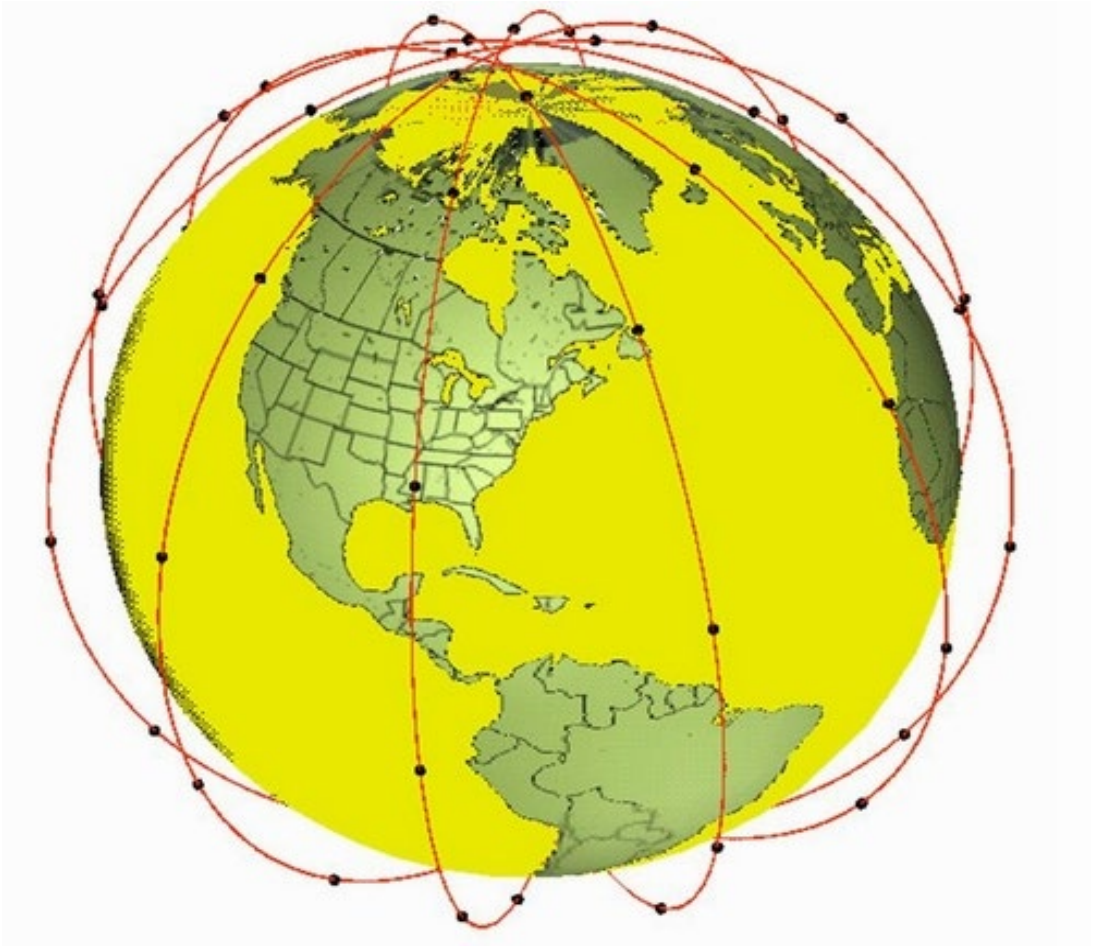

Figure 1: IRIDIUM Satellite Constellation

IRIDIUM has deployed two satellite constellations since it began operations. The first-generation IRIDIUM constellation was launched in 1997-1998, and operated until 2019. During 2017-2019, a replacement constellation - known as IRIDIUM NEXT - was launched to fully replace the first-generation, and these early satellites were subsequently decommissioned and deorbited. The IRIDIUM NEXT constellation architecture is identical to the first-generation, although the satellites themselves have significantly advanced in design and capability.

5.2 STRUCTURE OF IRIDIUM SIGNAL

IRIDIUM is designed to operate in up to 10.5 MHz of spectrum in the band 1616-1626.5 MHz and utilises time division multiple access (TDMA) technology for satellite access using bi-directional service link transmissions. At launch in 1998, the IRIDIUM system was initially authorised to operate within the band 1621.35-1626.5

MHz, but has additionally been authorised in the USA and a number of other countries worldwide to operate down to 1617.775 MHz. Within this band, the available spectrum is organised in sub-bands consisting of eight 41.667 kHz channels, each of which can be accessed individually or aggregated together.

IRIDIUM user terminals employ a time-division duplex (TDD) approach wherein they transmit and receive in an allotted time window within the frame structure. The TDD structure is built on a 90 ms frame and is composed of a 20.32 ms downlink simplex time slot, followed by four 8.28 ms up-link time slots and four 8.28 ms down-link time slots, with some guard times interspersed as is depicted in Figure 2. Since the system is using TDD, the subscriber units transmit and receive in the same frequency band (although not necessarily on the same channel). The access technology is a Frequency Division Multiple Access/Time Division Multiple Access (FDMA/TDMA) method whereby a subscriber is assigned a channel composed of a specific frequency and time slot in any particular beam. Channel assignments may be changed across cell/ beam boundaries (and across satellite handover) and are controlled by the satellite.

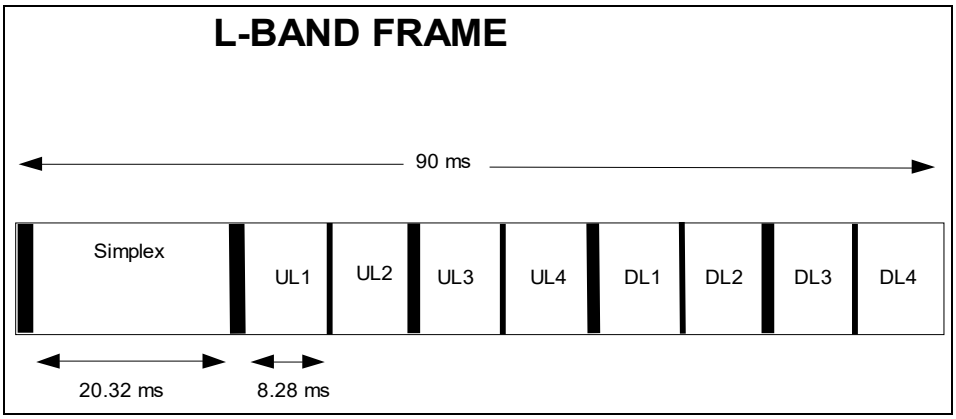

Figure 2: IRIDIUM Frame Structure

5.3 SATELLITE MODES TO REDUCE UNWANTED EMISSIONS

According to IRIDIUM, when designing the IRIDIUM NEXT satellites, one of the key objectives was to reduce the impact of unwanted emissions on the adjacent RAS allocation. The new satellites incorporated hardware features that were not available on the first-generation spacecraft, including:

- State-of-the-art hardware design and controls;
- Improved linearity of High-Power Amplifiers (HPAs);
- Surface Acoustic Wave (SAW) noise filters;
- Improvement in control of Transmit/Receive ("T/R") modules and their traffic loading.

The hardware improvements alone were expected to demonstrate an approximately 15 dB reduction in unwanted emissions, and when coupled with new beam management techniques were expected to reduce unwanted emissions in line with levels recommended in Recommendation ITU-R RA.769-2 [4].

Once the new constellation was complete, the initial set-up of the satellites (measured in April/May 2019) confirmed the potential to significantly reduce the impact to RAS, but resulted in significant operational problems that were unsustainable. Subsequently, IRIDIUM further developed and refined the satellite set-up using the capabilities of the new satellite design. This included the capability to select spectrum usage and transmit back-off power separately for each service type, allowing the use of channels to be optimised for minimal unwanted emissions.

The complexity of traffic management software, including anticipating its impacts on RAS protection, was evidenced by the operational problems encountered during 2019. As a result, further adjustments to the satellite set-up were extensively tested on simulators before being deployed incrementally across the constellation to reduce further operational impact. A new set-up was completed in mid-2020, and the resulting emissions measured by Leeheim. These measurements are described in section 6.

6 MEASUREMENTS OF IRIDIUM NEXT SATELLITES

6.1 DESCRIPTION OF LEEHEIM MONITORING STATION

The Leeheim Space Radio Monitoring Station is located approximately 35 km south-west of Frankfurt/Main.

The Leeheim MS has a number of satellite antennas including a 12 m parabolic reflector Antenna 1 designed to cover the 1-13 GHz frequency range, with which the monitoring was done. High-precision angular pointing allowed for accurate tracking of moving satellites. The relevant parameters of the Leeheim MS Antenna 1 are:

- Antenna type: Cassegrain;
- Dish diameter: 12 m;
- Aperture efficiency (including taper): 0.64;
- Polarisation: linear;
- Antenna gain: 44 dBi (1.5-1.8 GHz band);
- Figure of merit: 17 dB/K (1.5-1.8 GHz band);
- Zenith system temperature: 120 K at 1620 MHz (without stop band filter);
- Antenna tracking: programmable tracking using orbital elements;
- Measurement uncertainty: 1.6 dB r.s.s. error (95% confidence level);
- Band Reject Filter – Type: Wainwright Instruments GmbH;
- Filter Model Number: WRCD 1616/1627-1614/1630-70/16EE;
- Filter Reject Attenuation: 1616.0 to 1627.0 MHz / 70 dB minimum.

The elevation-dependence of antenna temperature T_{ant} has been carefully determined in 1980 at the time of antenna commissioning (Figure 3). The filter loss (Figure 4) is responsible for the majority of the system noise, only for elevations near the horizon, a significant contribution from the ground radiation can be expected. Combining these filter losses with the elevation dependent antenna temperature $T_{ant}(\phi)$, as interpolated from the measured values, yields the system temperature as a function of frequency and elevation:

$$T_{sys}(\nu, \varphi) = T_{ant}(\varphi) + T_{RX} + 290\,(L_1(\nu) - 1)$$

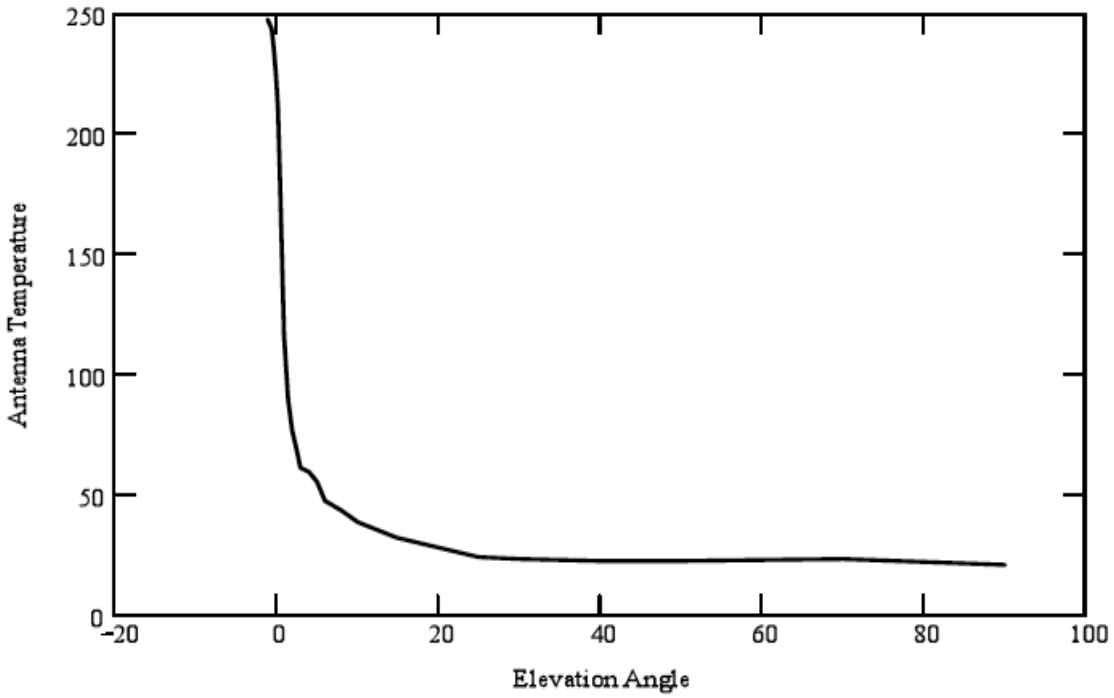

Figure 3: Leeheim antenna temperature as determined in 1980

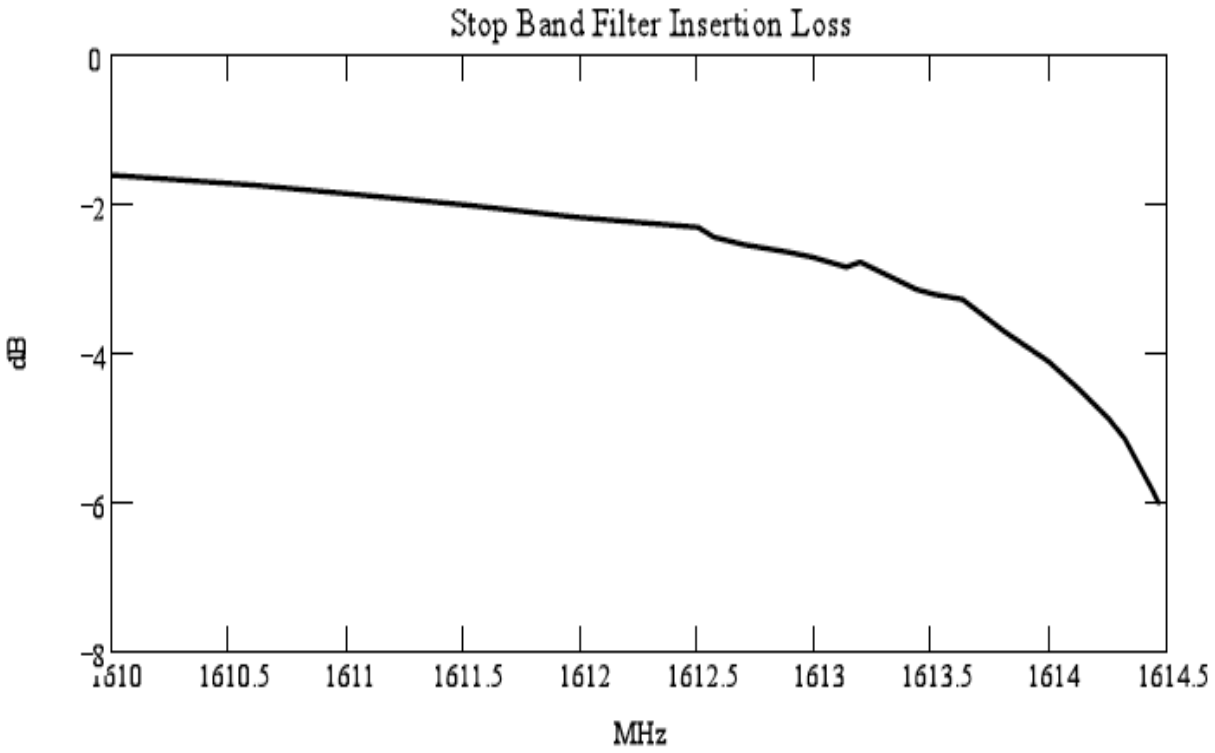

Figure 4: Insertion loss of the stop band filter

Figure 5 illustrates the expected behaviour of the system temperature for different elevations within the radio astronomical band.

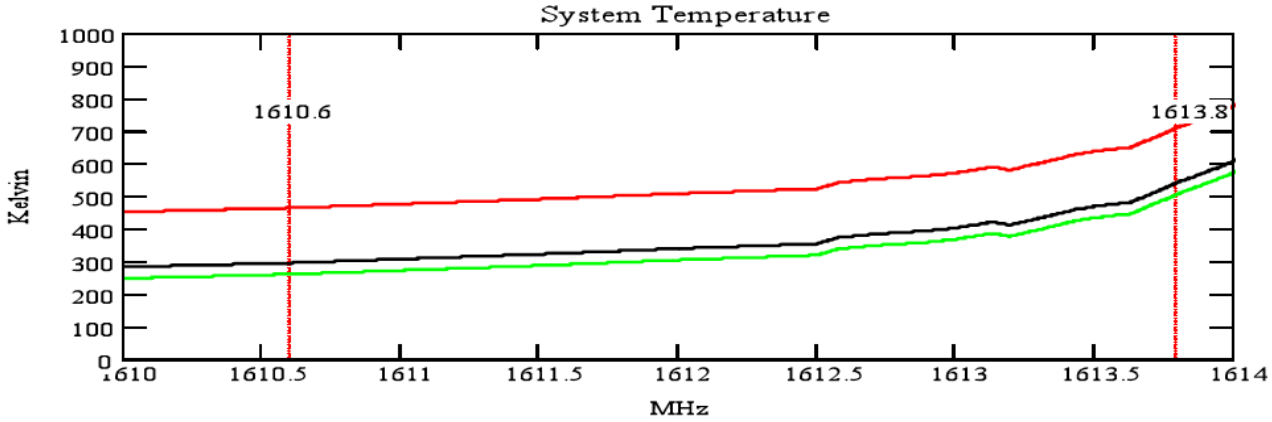

Figure 5: Total expected noise temperature for the Leeheim satellite tracking system used in the measurements. The green trace shows the expected system temperature at ϕ=90° (zenith), the black trace at ϕ=5° and the red trace at ϕ=0° (horizontal)

As the noise temperature of the Leeheim satellite tracking system varies with elevation, and this temperature provides one factor in the differential calculation for calibrating each measurement, it was recognised that a single noise temperature could not be used in the processing of measurement data. Instead, the noise temperature was characterised by elevation by measuring noise while tracking a simulated satellite “pass” pointing to blank sky[2]. The resulting curve was used to characterise system noise for each elevation – example shown in Figure 6:

[2] This was achieved by pointing to a location mid-way between two consecutive Iridium satelites in the same orbit, and tracking that location though a complete "pass".

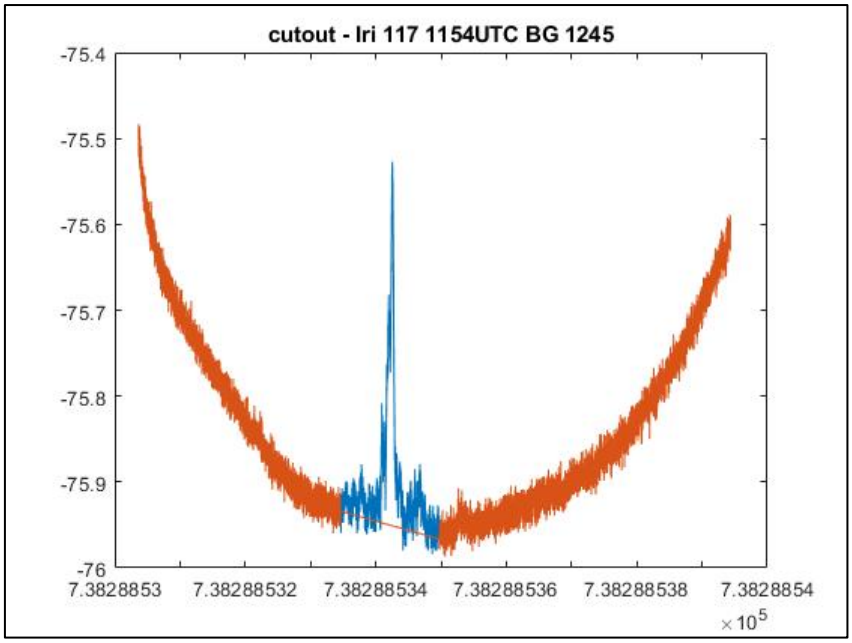

Figure 6: Characterisation of measurement system noise by elevation

(Note: The blue section of the curve was identified to have been impacted by localised noise/interference. Where this occurred, the affected section of the data was removed and replaced with a smoothed curve to ensure consistent calibration.)

Furthermore, because of the noise of the Leeheim measurement chain, the sensitivity is insufficient to assess data loss down to the 2% objective. In order to assess the maximum sensitivity of the measurement chain, data from the system noise measurements was processed in the same way as satellite measurements. This gave an indication of the minimum data loss measurement achievable by the measurement chain at that time. Typically this was of the order of 15-20%, and is shown in the results.

6.2 DESCRIPTION OF THE FFTS

Technical specifications of the dual channel real-time digitising and recording system:

- FFT: 4096;
- Digitisation: 16 bit;
- Output range: 256 dBm;
- Dynamic resolution: 0.0039 dBm (value ‘ydelta” in mat-files);
- Oversampling factor: 4/3.

Due to these specifications the following settings were chosen to match the required values:

- Internal bandwidth: 7.5 MHz;
- Bandwidth used for RAS band: 4 MHz;
- Sampling rate: ~1e-7 s;
- Averaging: 128.

This results in the following time and frequency resolution:

- Integration time: ~52.4 ms (value ‘duration’ in mat-files);
- Channel bandwidth: ~2.4414 kHz (value ‘xdelta’ in mat-files).

Time synchronisation:

- Antenna control unit: internal GPS receiver;
- Dual channel real-time digitising and recording system: Meinberg LANtime M300.

6.3 CALIBRATION PROCEDURE

The observing procedures used for all satellite measurements incorporated the well-established calibration procedures used in radio astronomy, as well as some adaptations to compensate for the limitations of the available equipment[3]:

1 Before each measurement session, a void satellite “pass” was measured to characterise the system noise temperature by elevation.

2 During each measurement session a strong celestial calibrator source, Cassiopeia A, was observed. This source, which has well-known power flux density in the band of interest, was used to calibrate the system bandpass across the RAS band and to provide the calibration scale from antenna temperature to absolute spectral power flux density in units of $Wm^{-2}Hz^{-1}$ for the satellite observations (Another source, Cygnus A, could also be used for this purpose as described below).

3 All satellite observations consisted of continuous tracking observations (from horizon to horizon) with a typical duration of 700 seconds followed by an observation of a blank sky position (antenna azimuth of 0° and elevation of 50°). The blank sky section of each observation was used to subtract the zero-level baseline from the tracking part of the data.

The celestial calibrator sources Cassiopeia A (size 4.3’) and Cygnus A (size 2’) have a known (calibrated) flux density and are unresolved by the Leeheim MS antenna beam (HPBW = 1.05°). The measured power at the antenna in mW per channel, which is a proxy for the antenna temperature, of the calibrator source directly determines scaling of the individual channels of the FFTS in astronomical flux density units given as 1 Jansky (Jy) = 10^{-26} $Wm^{-2}Hz^{-1}$. Cyg-A has a flux density of 1690±3 Jy at 1304 MHz and 1210±3 Jy at 1765 MHz [11]. Linear interpolation yields a flux density of 1371 ±5 Jy at 1610 MHz (interpolated flux density). Similarly, the flux density of Cas-A of 1476 Jy at 1610 MHz was used for the calibrations in this Report[4]. An example calibration measurement of Cygnus A is presented in Figure 7.

The shape of the bandpass across the RAS band is strongly affected by the stop-band filter in Figure 8 (left). A “spline fit” (interpolation) through the spectrum may be used to correct for this bandshape and produces a spectrum for Cyg-A as presented in Figure 8 (right). Using the system noise and the conversion efficiency of the antenna, 0.026 K/Jy one can calculate the system temperatures across the band and their range from 350 - 700 K is in good agreement with predictions derived from the system characteristics. After flattening of the bandpass of the measurement data may be converted to flux units using the conversion function (from antenna temperature to Jansky) shown in Figure 8 (right). Some strong and narrow interference was sporadically found in the data, which was ignored in subsequent data processing. In L-Band, the transmissions of IRIDIUM satellites exhibit right-hand circular polarisation. In the receiving system the circular signal is equally split into two linear signal components which thus have half of the energy. This 3 dB loss is compensated by the calibration with the extra-solar radio source Cassiopeia A. One linear signal path is equipped with a reject filter for in-band frequency signals of the IRIDIUM NEXT system and used for the unwanted emissions measurement. The other linear signal path is used for the comparison with the in-band signals.

3 Radio astronomy observatories typically employ specialist radio equipment and highly developed methods to minimise noise and maximise sensitivity. Some of these methods, such as cryogenically cooling the LNA, are not practical outside of an RAS observatory. As Leeheim is a satellite monitoring facility, it uses commercial-grade measurement equipment that is of a high-grade but ultimately not capable of the same degrees of sensitivity.

4 It is noted that the flux density of Cas-A changes over time. On a long-term average it gets dimmer by about 1% per year.

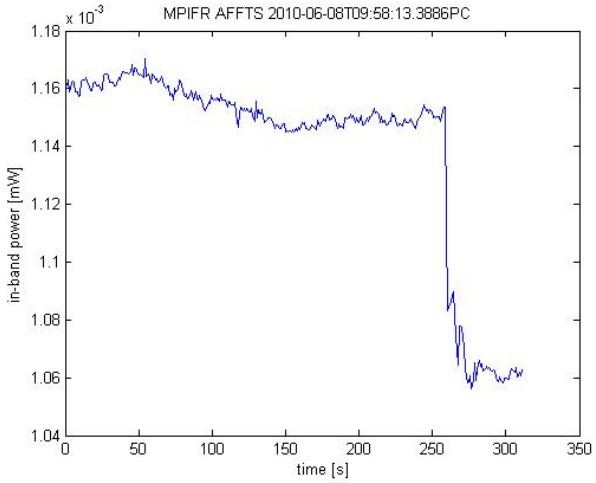

Figure 7: Example measurement of Cyg-A

Note: the Cygnus A source is present in the first 250 sec of the scan, followed by a background measurement at an antenna azimuth of 0° and elevation of 50°.

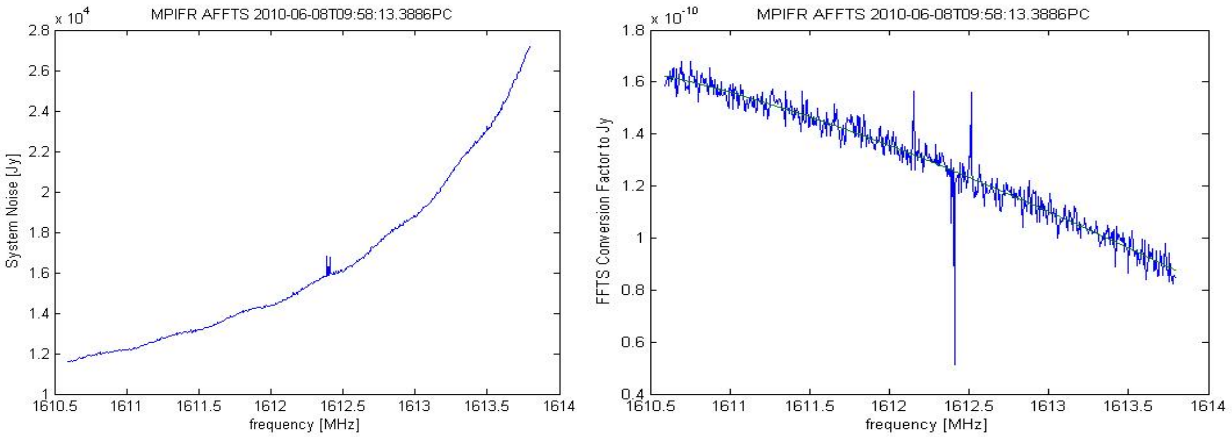

Figure 8: System noise and transfer function from calibration on Cyg-A

6.4 Characterisation of Elevation Dependence

Improvements in the software used for processing the data were introduced in the 2017-2019 period to take into account the elevation-dependence of critical factors in the measurements, in particular:

- Removal of the background noise due to the ground and atmosphere: a “void pass” (i.e. without pointing an IRIDIUM satellite) is recorded at the beginning of a measurement session to generate an average noise versus elevation estimate. After each measurement of an IRIDIUM satellite, the sky noise is measured at high elevation (typically 50°) and the average noise estimate is re-adjusted to compensate for a possible offset resulting from ambient condition changes in the time interval between the void pass and the satellite measurement. This corrects most of the elevation-dependent bias due to the ground noise effect, but does not remove the noise variations around the baseline. This residual noise component alone (i.e. without IRIDIUM satellite) when used in the simulation generates a significant apparent “data loss” that cannot be attributed to IRIDIUM;
- The consideration of elevation dependence of IRIDIUM satellite unwanted emissions: a fundamental assumption in the measurement campaigns in 2005, 2010 and 2013 was that satellite emissions produced a constant pfd on Earth regardless of elevation. However, this was subsequently found to be inaccurate as the satellite antenna tend to radiate less unwanted emission power at lower elevations compared to nadir. As a result, the software was amended in 2019 to take the elevation angle into account: the pfd of simulated satellite is extracted from satellites measured at a comparable elevation in the datasets, which

allows to have elevation-representative measurements without the need to make assumptions on the satellite radiation pattern (see Annex 2 for background information);

- Measurements for elevations below 10º were discarded entirely.

6.5 LEEHEIM MEASUREMENTS SESSIONS

In July 2020, IRIDIUM informed BNetzA Leeheim that the satellite constellation had been placed in a stable configuration, ready for measurements to be taken.

Table 3: Measurements during the period 30 November 2020 to 12 May 2021

Satellite	Slot	Period	Date	Time (CET)	max elev.	Threshold exceeded in % of measurement (before processing)	Channels with exceeded thresholds (before processing)
IRIDIUM 120 (day)	7	1	30.11.2020	13:03	71.6	5.4	164
IRIDIUM 120 (night)	7	1	09.12.2020	00:58	83.2	0.7	123
IRIDIUM 131 (day)	11	1	30.11.2020	13:40	57.9	5.2	164
IRIDIUM 131 (night)	11	1	09.12.2020	01:34	49.6	0.3	149
IRIDIUM 117 (day)	1	1	17.12.2020	14:18	49.4	0.7	164
IRIDIUM 117 (night)	1	1	09.12.2020	03:20	73.1	0.0	17
IRIDIUM 172 (day)	10	1	17.12.2020	14:00	70.3	1.3	164
IRIDIUM 172 (night)	10	1	09.12.2020	03:01	80.4	0.0	0
IRIDIUM 120 (day)	7	2	06.04.2021	13:51	81.0	3.5	164
IRIDIUM 120 (night)	7	2	26.03.2021	01:56	50.4	0.2	117
IRIDIUM 131 (day)	11	2	07.04.2021	13:49	86.2	2.2	164
IRIDIUM 131 (night)	11	2	26.03.2021	02:33	82.0	0.2	128
IRIDIUM 117 (day)	1	2	12.05.2021	14:28	73.6	0.0	66
IRIDIUM 117 (night)	1	2	30.03.2021	03:45	55.8	0.0	0
IRIDIUM 172 (day)	10	2	23.04.2021	14:43	61.9	0.0	96
IRIDIUM 172 (night)	10	2	30.03.2021	03:26	39.6	0.0	0

As requested, the satellites were selected from two adjacent planes (plane 2 and plane 3), and were measured during both night time and daytime to observe the variation in unwanted emissions due to traffic changes. The measurements were repeated a few months later. All passes were high elevation, as requested. However, traffic loading is different towards the east and west of Europe.

The two right-hand columns in Table 3 only inform about pre-processed data and should not be misinterpreted as the measurement results. It represents peak values of a single satellite passover.

These values are calculated before the correction for antenna noise. It should be noted that variation in the antenna noise alone can “exceed” the protection criteria and result in up to 20% “data loss”, if processed in the same way as measurement data. Antenna noise is removed in a later stage of the processing. Furthermore, the processing takes into account both the RAS antenna gain and the time variance of the unwanted emissions interference. The full processing software takes all the measurements of 16 individual satellites (in this campaign), builds a statistical unwanted emissions model, and then simulates the impact on a RAS station as if all visible satellites were generating those unwanted emissions. The simulation software samples the unwanted emissions model at each timestep, and then calculates the aggregate interference seen by the RAS antenna. However, the RAS antenna has a very narrow beamwidth (approx. 0.11º at -3dB) and so most unwanted emissions fall into the sidelobes and are attenuated. Given the narrow beamwidth, a satellite spends no more than a few seconds (at most) in the main lobe, and most often does not interest the beam at all. In these cases, the impact interference is reduced by the antenna isolation.

The simulation software calculates the aggregate impact by calculating the RAS antenna gain in the direction of each visible satellite. The simulation tool calculates the interference impact at each timestep, and then calculates an average over 2000 s to determine the data loss. Typically, this is repeated for 100 iterations for each pointing angle in the sky, and the results averaged over the entire sky for a single metric. Results are shown in section 7.

Leeheim tracks whether other possible sources of satellite interference in the band could impact the measurements. For example, in one measurement (Ir120 30.11.2020 13:09:47CET) a GLONASS satellite came close to the main lobe for some seconds with a minimal angular separation of 1.03 degrees. However, no signal could be detected. For the other measurements no GLONASS or GLOBALSTAR satellites came close to the main lobe of the antenna during the measurements.

It has to be noted that during the two monitoring periods a reduction in bandwidth on all satellites was observed when the satellite visibility was above a certain elevation. At low elevation angles, the use of the full frequency range 1618-1626.5 MHz for communication purposes was observed.

The RAS protection threshold in units of Janskies (Jy) depends on the integration time. Recommendation ITU-R RA.769-2 defines a threshold of -238 dB(W/m²/Hz) for an integration time of 2000 s, which is equal to 158 Jy. Shorter integration times result in reduced RAS sensitivity. The integration for the monitoring is limited by the time of visibility of a satellite under measurement during transit. For the listed measurements, the time is between 576 s and 627 s. This results in a thresholds of 299 Jy to 286 Jy. For a short observation time of 1 s, the threshold is 7004 Jy.

6.6 OBSERVATIONS ON RAS PROTECTION MODE OPERATION

A Radio Astronomy Service Protection mode configuration was in operation during the measurements.

IRIDIUM stated that such configuration will protect Leeheim and Effelsberg, as well as all other sites in Northern Europe.

IRIDIUM informed BNetzA about on-board tests of software modifications on four IRIDIUM NEXT satellites in the time period from 15-19 May 2021 and in the time period from 12 April to 3 May 2021 on further 7 different IRIDIUM NEXT satellites. No measurements from any of these satellites during the test periods were used in this Report.

It was observed that the IRIDIUM spectrum occupancy depends on the satellite position. In different in-band spectrograms (e.g. IRIDIUM-120 (night) 00:09 UTC) it has been observed that frequencies at the lower edge

are only used at low elevations. This was assumed to be part of the protection mode, as often corresponding unwanted emission increases or decreases. For further analysis of this behaviour, the spectrograms were evaluated manually in order to determine the point in time when certain frequency ranges were switched on or off.

Figure 9 and Figure 10 demonstrate how the evaluation was made. It shows in detail IRIDIUM-120 (night) with annotations.

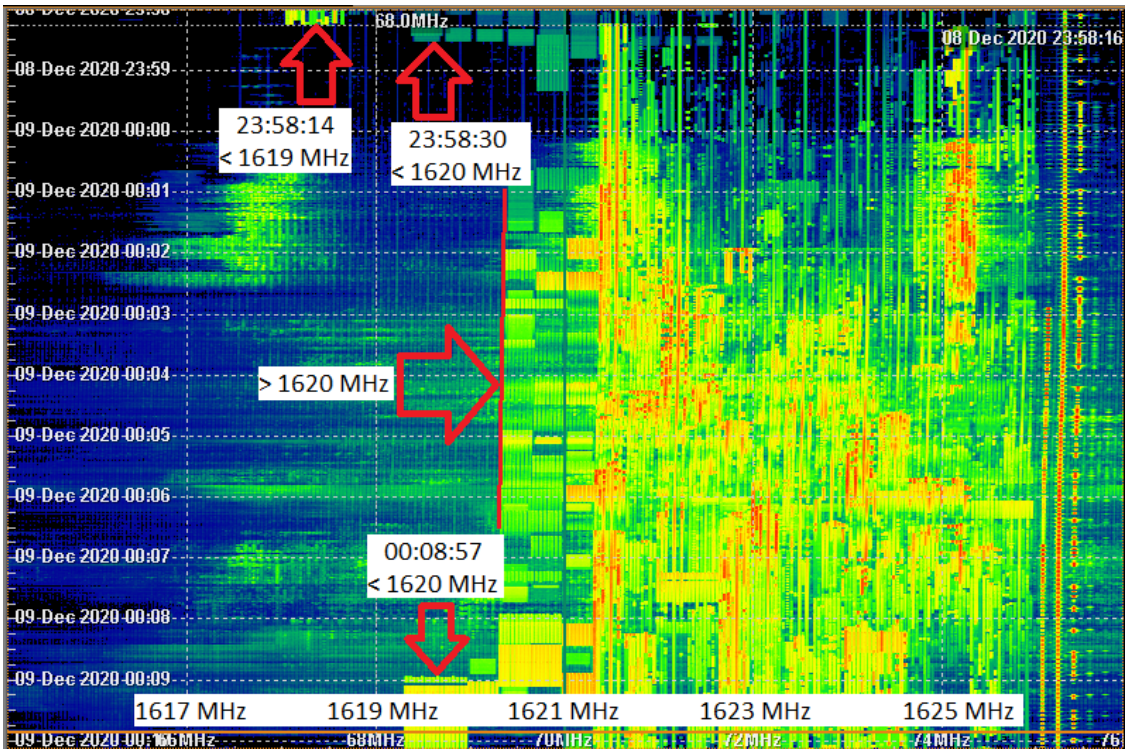

Figure 9: In-band spectrogram evaluation

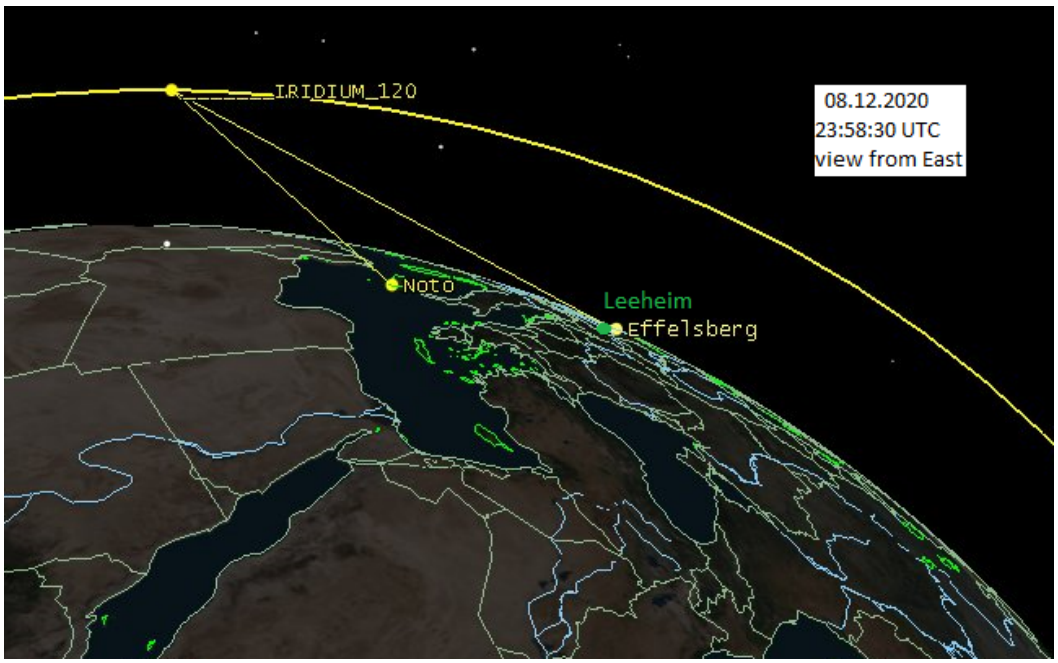

Figure 10: Example for satellite position when switching off frequencies below 1620 MHz

With the determined times, the sub-satellite positions were calculated and marked with the observed frequency range. The result is displayed in Figure 11.

The locations of CEPT radio astronomy stations shown in the map were taken from the CRAF website.

Only radio astronomy stations which make use of the frequency band 1610.6 to 1613.8 MHz are shown.

Note: For all other calculations in the report only values were taken into account that were measured at elevations above 10°.

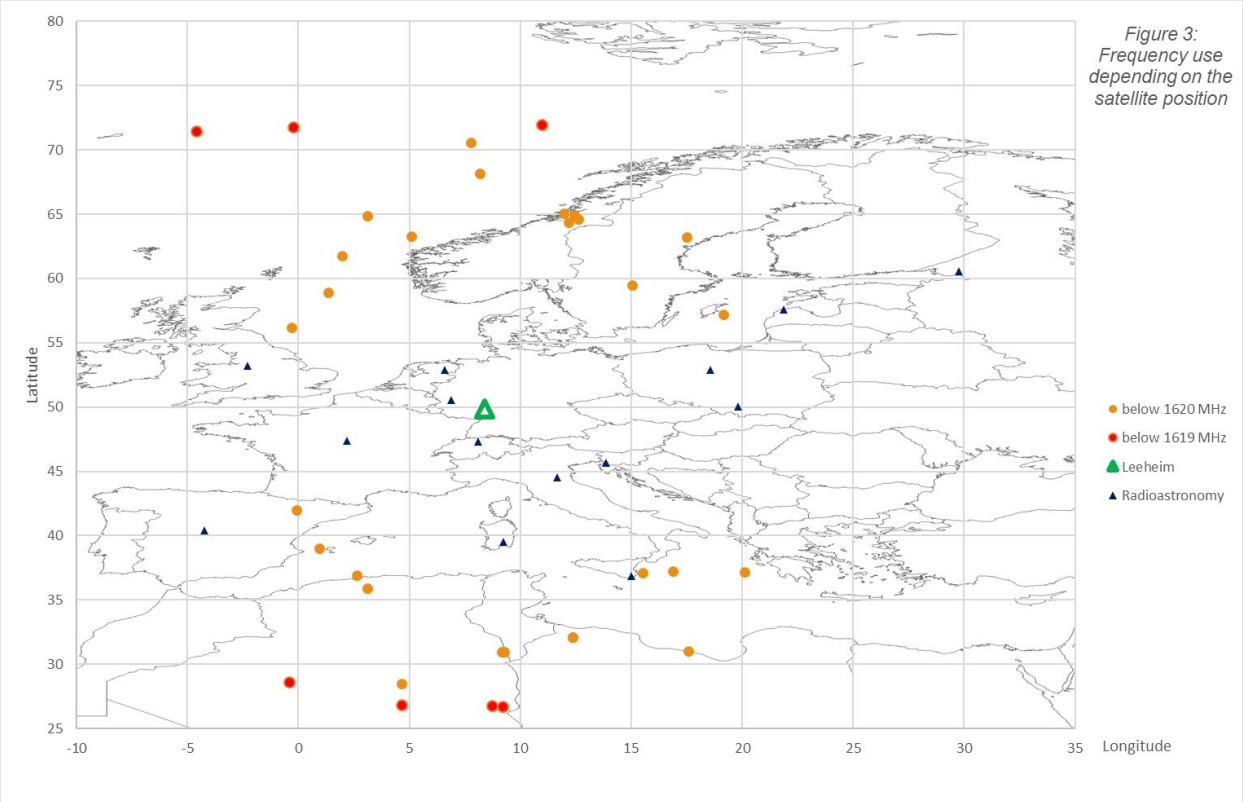

Figure 11: Frequency depending on the satellite position

IRIDIUM advised that the frequency range is one of several elements in their satellite management "toolkit" used to control unwanted emissions. It is the only one that can be directly observed from measurements on the ground, but other elements that contribute to the reduction of unwanted emissions are present but not directly observable. These include the arrangement and grouping of services within the band, power control, and slot assignment. It cannot be assumed that areas where a wider band is used correlate with higher unwanted emissions, since these emissions are predominantly driven by the high traffic levels typically experienced in continental Europe. In the case shown in Figure 10, the two locations correspond to separate satellite beams and therefore unwanted emissions may not be correlated. The definitive method of determining unwanted emissions is to measure them directly, which is the focus of this Report.

6.7 EPFD methodology and results

The measurements performed during 30 November 2020 and 12 May 2021 were processed using the procedures described in sections 6.1 to 6.4 (see also ECC Report 247 [9]). After performing these procedures on the 16 datasets provided, none of the datasets were excluded for the epfd calculation.

Cumulative distribution functions were generated to model the interference power levels from each of the measured satellites. Figure 12 and Figure 13 presents the distributions for the highest channel of the measured

band centred at frequency 1613.7878 MHz, and the equivalent results from measurements in 2013 [8] for comparison.

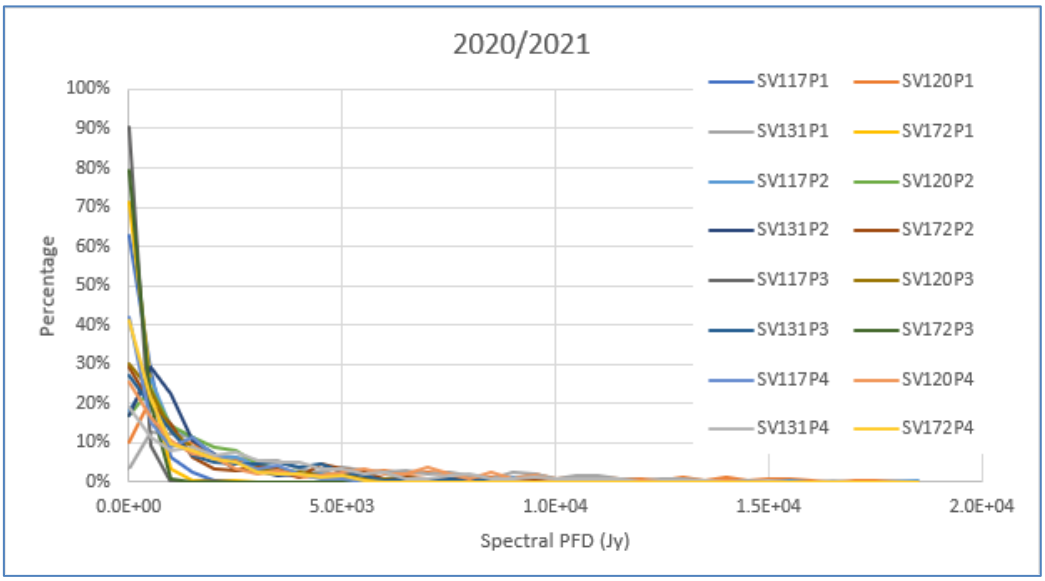

Figure 12: Cumulative distribution functions for the satellites of the 2020/21 measurements campaign

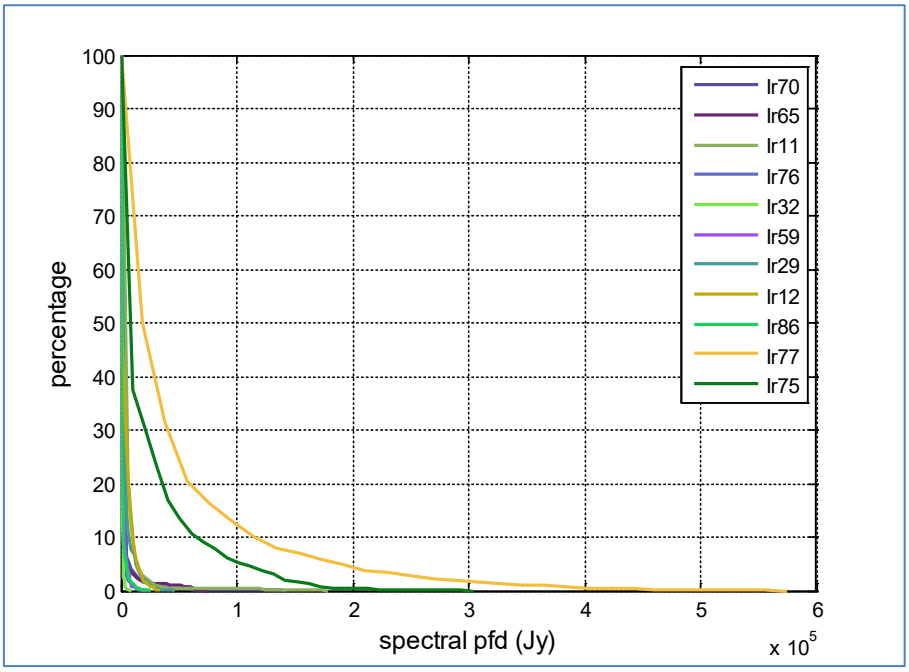

Figure 13: Cumulative distribution functions for the satellites of the 2013 measurements campaign ([8])

As can be seen, the highest emission levels are reduced by an order of magnitude from the CDF results in 2013.

The generated distributions were used as input data for the simulation tool to carry out the epfd calculations, using the methodology described in Recommendation ITU-R M.1583 [2].

The variation of the data loss (in percentage) across the sky for the frequency channel 1610.6267 MHz at the lower edge of the RAS frequency band is presented in Figure 14 and the equivalent result also shown in Figure 15 for the 2013 measurements [8] for comparison:

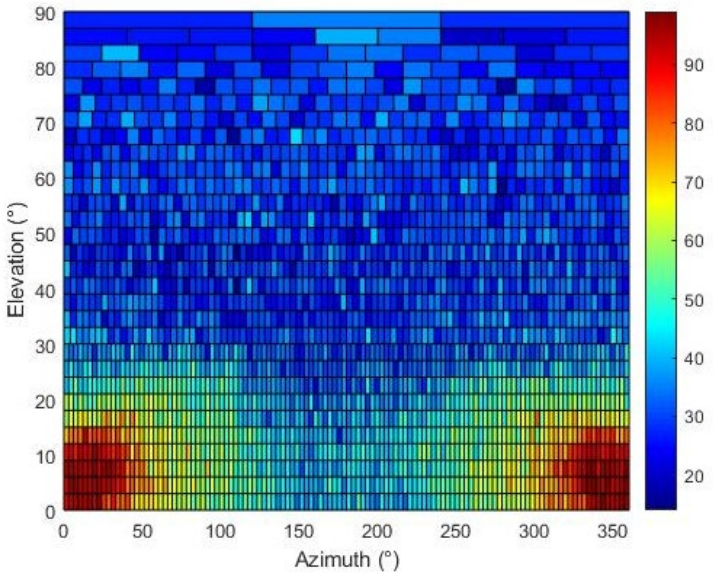

Figure 14: Variation of the data loss (in percentage) across the sky at frequency 1610.6267 MHz, 2020/21 measurements

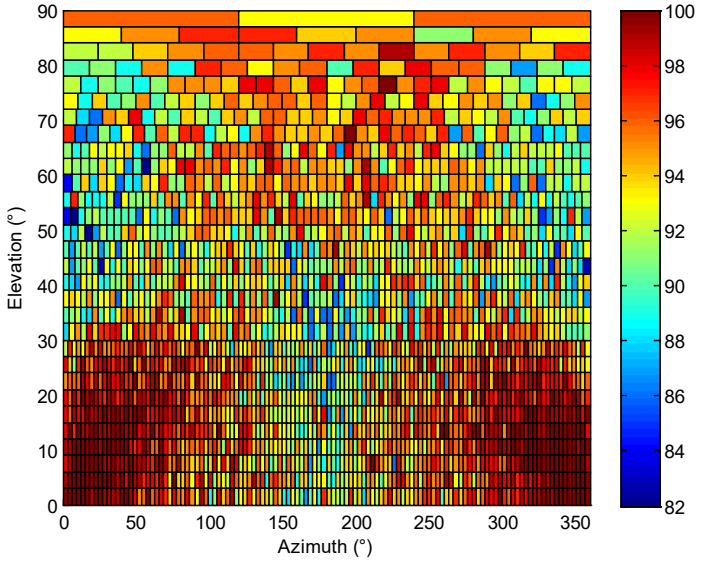

Figure 15: Variation of the data loss (in percentage) across the sky at frequency 1610.6267 MHz, 2013 measurements

The overall data loss in 2020/21 is found to be 18.8% (c.f. 94.4% in 2013) when considering an integration time of 2000 seconds. In order to meet the 2% criterion, the simulation estimated that the average interference power level should be reduced by 5.1 dB (c.f. 22.8 dB). Noting the change in scale between the two data sets, the overall reduction in data loss is clearly obvious.

For the frequency channel at the highest edge of the RAS frequency band (1613.7908 MHz) the overall data loss across the sky is found to be 82.5% (c.f. 100%), when considering an integration time of 2000 seconds. In order to meet the 2% criterion, the simulation estimated that the average interference power level should be reduced by 9.1 dB (c.f. 32.3 dB).

7 ASSESSMENT OF IRIDIUM NEXT IMPACT TO RAS

The satellite unwanted emissions data collected by BNetzA Leeheim during 2020/21 was examined and processed following the procedure described in ECC Report 247 [9]. The results are shown on Table 4, together with the results of previous campaigns.

Table 4: Results of IRIDIUM NEXT measurement campaigns

	Nov. 2013		April/May 2019		Oct./Nov. 2019			Nov. 2020/ May 2021
	Data loss	DEC (dB)	Data loss	DEC (dB)	Data loss	DEC (dB)	Data loss	DEC (dB)
Measurement	IRIDIUM + Noise							
1613.8 MHz	*	*	48.00%	18.7	100%	31.8	99.90%	24.7
1610.6 MHz	*	*	26.40%	15.7	100%	24.7	37.20%	16.7
Noise	Noise							
1613.8 MHz	*	*	18.70%	15.7	15.60%	18.2	17.50%	15.7
1610.6 MHz	*	*	21.70%	16.7	7.20%	10.1	18.50%	11.6
Result	IRIDIUM							
1613.8 MHz	100%	32.3	29.30%	3	84.40%	13.6	82.50%	9.1
1610.6 MHz	94.4%	22.8	4.70%	-1	92.70%	14.6	18.80%	5.1

* In 2013, Leeheim did not take noise measurements to compensate for elevation-variable antenna noise.

In addition to the estimate of data loss, a DEC value shows the estimated further reduction in unwanted emissions that would be necessary to achieve the target 2% data loss. To overcome the limitations in sensitivity, data loss and DEC values were calculated for the system noise (using the void satellite passes) and these were subtracted from the measurement results.

Table 4 shows results for four different measurement campaigns, beginning with the first-generation constellation (2013 [8]) and then the second-generation satellites under different operating settings (April 2019, October 2019 and May 2021). IRIDIUM reported that the settings used in April 2019 were too restrictive for their operations; measurements taken in October 2019 reflect the situation with restrictions removed. New operational restrictions were implemented in May 2020, and were in place when the most recent measurements were taken.

The results show, in regard to the reduction of unwanted emissions, an improvement over the results from October/November 2019, but they are still less satisfactory compared to the measurements made in April/May 2019 (when IRIDIUM had significantly reduced traffic on satellites in the vicinity of European RAS stations, such as Effelsberg). It should be noted that ECC Report 247 [9] concludes that “because of the noise of the measurement chain, it may not be possible to assess data loss performance down to the 2% objective”. Therefore, “in order to assess the sensitivity of the measurement chain, users may use data taken from several ‘void satellite passes’, i.e. without pointing towards IRIDIUM satellites, and assess data loss on that basis”. By comparing the data loss values of the results of the EPFD simulation for both cases (i.e. with and without IRIDIUM signals, both subject to receiver noise), one can infer the actual impact of the satellites alone. The same can be done for the so-called DEC parameter, which is the estimated attenuation of the interference level needed to reach the 2% target.

It is noted that the data loss (percentage) and the DEC value (dB) are not linearly related, due to the fact that "data loss" is defined as a binary outcome. Interference above the threshold, after averaging over the reference 2000 s time period, is classified as a "data loss" event, regardless of whether the exceedance is 0.1 dB or 20 dB. As average emissions are reduced close to the threshold, the data loss has been shown to fall more significantly. The DEC metric was therefore considered a more effective measure of exceedance.

ANNEX 1: SCALING OF INTERFERENCE LIMITS GIVEN IN RECOMMENDATION ITU-R RA.769

Thermal noise has a Gaussian distribution $p(u,u_0)$ of amplitudes, characterised by its rms amplitude u_0:

$$p(u,u_0) = \frac{e^{-\frac{u^2}{2\,u_0{}^2}}}{\sqrt{2\pi}\cdot u_0}$$

As a result, the distribution of noise power w, with average power w_0, is that of the squares of amplitudes given by a γ-distribution:

$$p_\gamma(\alpha,\beta,w) = \frac{\beta^\alpha w^{\alpha-1} e^{-\beta w}}{\Gamma(\alpha)}$$

with $\alpha=1/2$ and $\beta=1/2w_0$. The γ-distribution is not symmetric and defined only for positive values of $\mu = \alpha/\beta = w_0$. The mean of a γ-distribution is and its variance is $\sigma = \alpha/\beta^2 = 2.w_0^2$ and yields the familiar $2^{1/2}$ factor for the calculation of the standard deviation of from the average noise power.

One can show that the averages x of N noise power measurements also follow a γ-distribution given

$$p_\gamma(\frac{N}{2},\beta,x) = \frac{x^{\frac{N}{2}-1}\beta^{\frac{N}{2}} e^{-\beta x}}{\Gamma(\frac{N}{2})}$$

The mean value is given by α/β which evaluates to w_0 as expected for $\alpha=N/2$ and $\beta=N/2w_0$, but the variance $\sigma^2 = \frac{2}{N} w_0{}^2$ is linearly decreasing with the number of noise power measurements.

Hence the standard deviation Δ_N for the average of N independent noise measurements is given by

$$\Delta_N = \sqrt{\frac{2}{N}}\cdot w_0$$

The Nyquist-Shannon sampling theorem states that a function that contains no higher frequency components than ν, is fully defined by sampling τ_s

$$\tau_s = \frac{1}{2\,\Delta\nu}$$

and the number of independent measurements that are averaged over an integration time t_{int} is then

$$N = \frac{t_{int}}{\tau_s} = 2\,\Delta\nu\, t_{int}$$

Using this result in the expression for Δ_n gives $\Delta_N = \frac{w_0}{\sqrt{\Delta\nu\cdot t_{int}}}$

or more familiar as the sensitivity according to Recommendation ITU-R RA 769-2, annex 1, equation 1:

$$\Delta_N/w_0 = \Delta P/P = (\Delta\nu\,.\,t_{int})^{-1/2} \qquad (1)$$

Where:

- P and ΔP: power spectral density of the noise;
- $\Delta\nu$: measurement bandwidth;
- t_{int}: integration time.

P and ΔP in equation (1) can be expressed in temperature units through the Boltzmann's constant, k:

$$\Delta P = k\,\Delta T \quad \text{and} \quad P = k\,T$$

Recommendation ITU-R 769-2, tables 1 and 2 [4] provide a convenient access to the interference limits calculated from the radiometer equation (e.g. t_{int} = 2000 s, ν = 1612 MHz and a measurement bandwidth $\Delta\nu$ = 20 kHz):

- Columns 3 and 4 give typical receiver (T_R= 10 K) and antenna temperatures (T_A=12 K), together yielding a system temperature T_{sys} = 22K;
- Using the radiometer equation (1) for the temperature sensitivity $\Delta T = (T_A + T_R)(\Delta\nu.t_{int})^{-1/2}$ yields the entry of 3.479 mK in column 5;
- Multiplication with the Boltzmann constant and division by the measurement bandwidth $\Delta\nu$ gives the system sensitivity in terms of power spectral density:

  ΔP = -253.2 dB(W/Hz) listed in column 6.

- The interference limit is set to be 10 dB below the sensitivity and the product with the observation bandwidth gives the input power limit in column 7:

  $\Delta P_H = \Delta P + 10 \log(\Delta\nu/\text{Hz}) - 10 = -220.2$ dB(W).

The power flux density $S_H\Delta\nu$ in column 8 is obtained through division by the isotropic antenna $c^2/4\pi\nu^2$ area and is explicitly given by:

$$S_H \Delta\nu = \Delta P_H - 10\log\left(\frac{c^2}{4\pi\nu^2}\cdot m^{-2}\right) - 10 = -194.6 \text{ dB(W/m}^2\text{)}$$

Note that $S_H\Delta\nu + 145.7$ yields the field strength threshold in dB(µV/m)

- The last column (9) gives the emission limit in terms of spectral power flux density (spfd) and can be had by simply omitting the bandwidth term in the equation above:

$$S_H = \Delta P - 10\log\left(\frac{c^2}{4\pi\nu^2}\cdot m^{-2}\right) - 10 = -237.6 \text{ dB(Wm}^{-2}\text{Hz}^{-1}\text{)}$$

Note that the conversion to the radio astronomical unit of Jansky is achieved by adding 260 to the value in column 9. Hence the spectroscopy limit for 2000 s integration at 1420 MHz is equivalent to 22.4 dB(Jy) or 174.5 Jy.

It follows from eqn. 1 and the derivation of the table entries that changes in the measurement bandwidth δf are to be treated in the same manner as changes in integration time t_{int}:

$$S_{769} = 10^{\frac{-238+260}{10}} \cdot \sqrt{\frac{2000\,\text{s}}{t_{int}} \cdot \frac{20\,\text{kHz}}{\delta f}}$$

ANNEX 2: ELEVATION-DEPENDENT PFD DISTRIBUTIONS FOR THE EPFD SIMULATION

The transmitted satellite power is subject to two effects, which have impact on the received emission at the satellite monitoring station, both of which depend on the elevation of the satellite to first order:

a) the effects of distance on the signal attenuation;

b) the relative gain of the elementary elements of the array in the station direction.

In the original epfd software, the measured pfd values were used to produce pfd distributions for the epfd simulation, without accounting for any of the above effects. With the generation-one IRIDIUM satellites, where the signals were very bright, these effects could be neglected. However, with the IRIDIUM NEXT constellation, the unwanted emissions pfd values are much closer to the sensitivity limit of the Leeheim station and demand for a more thorough data processing.

The "roll-off" curve, which describes the effective satellite antenna gain with satellite elevation (as seen from the receiver), is shown in Figure 16.

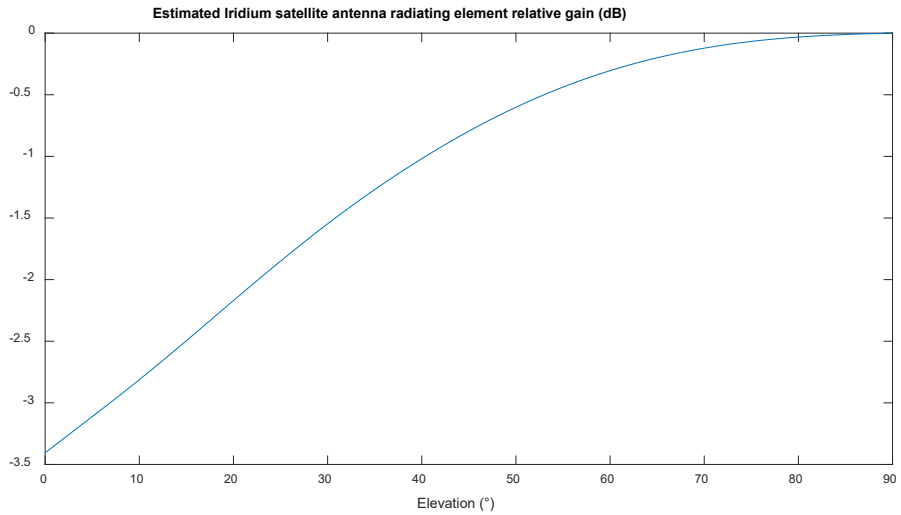

Figure 16: Satellite "roll-off" curve describing the IRIDIUM antenna element gain vs. elevation

In a first attempt, the measured pfd values were multiplied with the inverse of the roll-off curve and the spreading loss (depending on elevation) to estimate the zenith e.i.r.p. distributions. In the epfd simulation, the zenith e.i.r.p. values were then again multiplied with the roll-off factor for each satellite and the spreading loss depending on its elevation. This, however, created a problem at very low elevations where the IRIDIUM interference is barely detected such that the roll-off curve amplified the noise instead. This had significant impact on the epfd results and in fact led to a situation where a measurement track would create high data losses even with no satellite in the data. While part of this issue could be in part circumvented with the introduction of the DEC metric (compare section 7), there were still doubts about the validity of this approach from a methodological point of view.

Subsequently, it has been proposed to use a different approach, in which elevation-representative pfd values can be obtained by binning the measured data into elevation sets. All recent measurement campaigns have observed a sufficiently large number of satellites, therefore each elevation bin could be filled with a data population from all measured satellites to get a representative set of pfd values. During the simulation, for a satellite at a given elevation, the corresponding pfd value is then drawn randomly from the measurements corresponding to a similar elevation range (elevation bins of 3° are suggested).

This "Elevation-dependent pfd" method is very similar to the original pfd method since measured pfds can be used directly in the simulation without correction factors (potentially distorting the distribution statistics). The only difference is that in the original pfd method, the simulated pfd for a satellite is randomly drawn from the full ensemble of pdf measurements, neglecting elevation completely.

ANNEX 3: LIST OF REFERENCES

[1] ITU Radio Regulations, Volume 1 - Articles, Edition of 2020

[2] Recommendation ITU-R M.1583: “Interference calculations between non-geostationary mobile-satellite service or radionavigation-satellite service systems and radioastronomy telescope sites”

[3] Recommendation ITU-R S.1586: “Calculation of unwanted emission levels produced by a non-geostationary fixed-satellite service system at radio astronomy sites”

[4] Recommendation ITU-R RA.769: “Protection criteria used for radio astronomical measurements”

[5] Recommendation ITU-R RA.1513: “Levels of data loss to radio astronomy observations and percentage-of-time criteria resulting from degradation by interference for frequency bands allocated to the radio astronomy service on a primary basis”

[6] ECC Decision (09)02: “The harmonisation of the bands 1610-1626.5 MHz and 2483.5-2500 MHz for use by systems in the Mobile-Satellite Service” approved 26 June 2009, amended November 2012

[7] ECC Report 171: “Impact of unwanted emissions of IRIDIUM satellites on radioastronomy operations in the band 1610.6-1613.8 MHz”, approved October 2011

[8] ECC Report 226: “Unwanted emissions of IRIDIUM satellites in the band 1610.6-1613.8 MHz, monitoring campaign 2013”, approved January 2015

[9] ECC Report 247: “Description of the software tool for processing of measurements data of IRIDIUM satellites at the Leeheim station”, approved January 2016, amended October 2020

[10] Annex 5 of SE40(19)017, WGSE Project Team SE40 to SAT MoU: "Requested measurements on Operational IRIDIUM NEXT constellation

[11] Baars et al., Astronomy and Astrophysics, 61, 99-106, 1977

[12] Recommendation ITU-R RA.314: “Recommendation ITU-R RA.314”